

# Process Development and Hot-fire Testing of Additively Manufactured NASA HR-1 for Liquid Rocket Engine Applications

Paul R. Gradl<sup>1</sup>, Thomas Teasley<sup>2</sup>, Chris Protz<sup>3</sup>, Colton Katsarelis<sup>4</sup>  
*NASA Marshall Space Flight Center, Huntsville, AL 35812*

Po Chen<sup>5</sup>  
*Jacobs Engineering, NASA Marshall Space Flight Center, Huntsville, AL 35812*

Additive manufacturing (AM) has provided new design and manufacturing opportunities to reduce cost and schedules, consolidate parts, and optimize performance. One technique being evaluated is Laser Powder Directed Energy Deposition (LP-DED), which provides a significant increase in scale compared to Laser Powder Bed Fusion (L-PBF). NASA along with industry partners have been developing the LP-DED process to demonstrate internal channel geometry and development components for use in liquid rocket engine channel cooled nozzles. Optimized materials in the extreme high pressure and hydrogen environment for liquid rocket engines remains a key challenge. NASA has advanced an enabling material called NASA HR-1 (Hydrogen Resistant -1) as a solution using AM techniques. NASA HR-1 is a high-strength Fe-Ni superalloy designed to resist high pressure, hydrogen environment embrittlement, oxidation, and corrosion. NASA HR-1 meets materials requirements for liquid rocket engine components, including good hydrogen resistance, high conductivity, good low cycle fatigue performance, and high elongation and strength for components in high heat flux environments. Material properties and process characterization have been completed on the high density thin-wall material in addition to advancements of the supply chain. NASA has also completed fabrication of several subscale and full-scale channel wall nozzles in LP-DED NASA HR-1 and completed hot-fire testing. This includes refinement of the process to produce thin-walls and various channel geometries to meet the requirements for channel wall nozzle applications. This paper will provide an overview of the LP-DED process development, material characterization and properties, component manufacturing, and hot-fire testing. Hot-fire testing was completed for a lander-class 7K-lbf thrust chamber using Liquid Oxygen (LOX)/Methane. The design overview and results from hot-fire testing will be presented in addition to hardware development for future testing on 2K-lbf and 35k-lbf thrust chambers and large-scale manufacturing technology demonstrators.

## I. Nomenclature

AM	=	Additive Manufacturing or Additively Manufactured
A <sub>x</sub>	=	Thermal processing aging cycle number
CH <sub>4</sub>	=	Methane
DED	=	Directed Energy Deposition
GHe	=	Gaseous Helium
h or hrs	=	hours
HIP	=	Hot Isostatic Pressing

<sup>1</sup> Senior Combustion Devices Engineer, Component Technology Branch, AIAA Associate Fellow

<sup>2</sup> Combustion Devices Engineer, Component Technology Branch, AIAA Member

<sup>3</sup> Team Lead, Component Technology Branch

<sup>4</sup> Materials Engineer, Metallics Branch

<sup>5</sup> Principal Scientist, Metallics Branch

HP	=	High Deposition Rate Plate (2620W 0.25” thickness)
K-lb <sub>f</sub>	=	thousand pound-force (thrust)
MSFC	=	George C. Marshall Space Flight Center
MTD	=	Manufacturing Technology Demonstrator
MP	=	Medium Deposition Rate Plate (1070W 0.140” thickness)
MR	=	Medium Deposition Rate Round Bar (1070W)
NASA HR-1	=	NASA Hydrogen Resistant Alloy (Fe-Ni-Cr)
L-PBF	=	Laser Powder Bed Fusion
LCF	=	Low Cycle Fatigue
LOX	=	Liquid Oxygen
LP	=	Low Deposition Rate Plate (350W 0.047” thickness)
LP-DED	=	Laser Powder Directed Energy Deposition
P <sub>c</sub>	=	Chamber Pressure (psig)
psig	=	Pounds Per Square Inch, gage pressure
T	=	Thickness
TCA	=	Thrust Chamber Assembly
W	=	Watts

## II. Introduction

Metal additive manufacturing (AM) has been demonstrated as an ideal technology to reduce the cost and lead time associated with fabrication of complex shapes with internal features. The technology is radically changing the design and manufacturing of liquid rocket engines components such as injectors, combustion chambers, nozzles, valves, and other fluid and structural systems. While AM is continuing to evolve, it is still in its infancy and over the past 10 years the materials available have been limited. As AM is considered for a design application, the designer has been forced to use the limited available materials, which may not be the optimal material for performance. The National Aeronautics and Space Administration (NASA) has identified the need to develop and advance new materials in unique engine applications such as hydrogen environments. One such material being developed is NASA HR-1. NASA HR-1 is a high-strength Fe-Ni superalloy designed to resist high pressure, hydrogen environment embrittlement, oxidation, and corrosion.

Combustion device components on liquid rocket engines operate in extreme environments that challenge the functional design, materials, and fabrication as part of an engine system. These components include combustion chambers, nozzles, injectors, gas generators, and igniter systems. Each of these components serve different functions, but have commonality in requirements. They must endure high pressure propellants and gases at high and low temperatures, while maintaining positive structural margins and allowing for a design with minimal mass in the engine system. Many of these components include complex internal features that provide complex flow passages, orifices, and small restrictions to provide proper mixing and cooling of the propellants and hot gases. The design of these components often require thin-walls and a combination of materials that must survive in these environments for multiple restarts.

The materials used in these applications must be selected for these harsh environments that include oxidation, hydrogen embrittlement, hydrocarbon coking, high pressure, high heat fluxes and high thermal gradients, and high static and dynamic loads. These materials must ensure compatibility with the propellants and also function under high and low cycle fatigue conditions to withstand engine and ambient environment loads for multiple use/restart applications. In addition, these materials will need to provide a high repeatability in component performances under these harsh conditions. For example, leaking hardware has been demonstrated to reduce global performance metrics in liquid rocket engines such as characteristic exhaust velocity and effectiveness of cooling for actively cooled hardware. These requirements translate into a material that requires high conductivity, high strength, high ductility, and high fracture toughness. A single alloy does not fit all of these requirements, so various alloys must be used as part of the design to optimize for the environment but also to minimize weight so the engine system can meet performance requirements for the vehicle mission. While many of these requirements are desirable for the end application, many must be translated into manufacturing and fabrication of the component and are not always practical or even possible.

The regeneratively-cooled, or channel-cooled nozzle, is a key component in various engine systems that expands combustion gases and increase the exhaust gas velocity. The cooled nozzle is often the largest structure on the liquid rocket engine, but must also maintain small internal channels for proper cooling of the hot-wall to maintain adequate structural margins. The design is balanced among extreme temperature environments, high pressure fluids, and

structural loads from thrust and sideloads during startup and shutdown. A common heritage design for regeneratively-cooled nozzles is the use of brazed tubes, but this technique presents challenges in the lead time of piece-parts, tube-stacking and assembly operations, brazing, and tooling [1]. The manufacturing of the large channel wall nozzles have been explored using various technologies including hot isostatic pressing (HIP) assisted brazing, laser welding, plating, and laser wire direct closeout [2,3]. NASA and other organizations have discussed the use of AM and advanced manufacturing techniques to solve some of the traditional manufacturing challenges for combustion chambers [4,5,6] and nozzles [7,8]. Many of these techniques focus on the reduction in cost and schedule for fabrication, but have also put an emphasis on increasing the scale, specifically AM technology.

There are specific needs identified based on channel wall nozzle requirements. With the common use of hydrogen for liquid rocket engines, a high strength compatible metal alloy is required that allows for ease of manufacturing and processing. Another need is the ability to fabricate large scale hardware not limited by existing machines, such as laser powder bed fusion (L-PBF). This paper addresses the development of the NASA HR-1 alloy, a hydrogen-resistant material, the process development using laser powder directed energy deposition (LP-DED), process maturity and scale-up, and hot-fire testing demonstration of hardware.

### III. LP-DED Process and NASA HR-1 Material Overview

#### A. Laser Powder Directed Energy Deposition Process Overview

The laser powder directed energy deposition (DED) process uses concentrated thermal energy, achieved with a laser, to fuse metals by melting locally as they are deposited [9]. This process allows for freeform fabrication of components or addition of material to components for the purposes of coating, repair, or modification using local deposition. Freeform components are formed by the precise control of various parameters that create individual (weld) beads that are deposited integrally to take a final geometric shape. LP-DED uses powder feedstock as the filler material and a laser as the energy source. The powder and laser optics are mounted on an integrated deposition head, which allows for the convergence of the laser and powder at a defined focus at the surface of the substrate where material melts and deposition take place. This substrate can be a sacrificial build plate or existing component. The deposition head is mounted to a robotic arm or gantry system to control the motion through programmed or logic toolpaths to deposit material or create features. An example of the process can be seen in Figure 1.

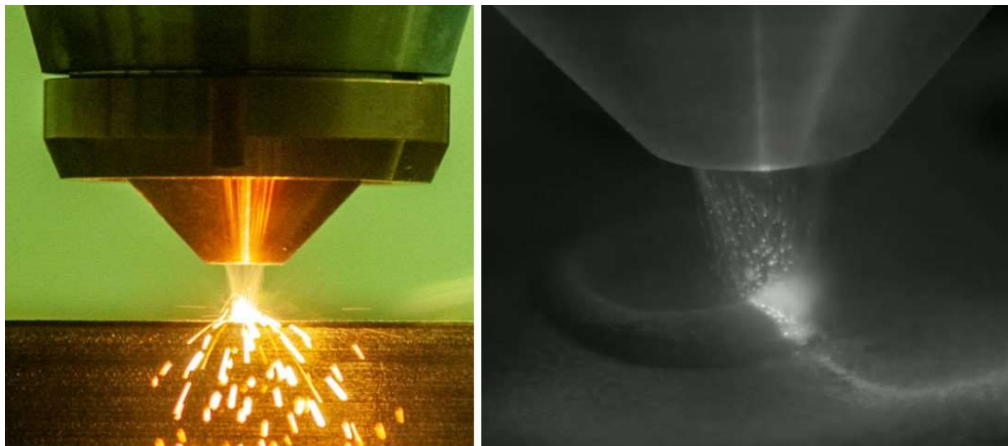


**Figure 1. Material being deposited using LP-DED.**  
[Left: Courtesy of AddUp, Right: Courtesy of Formalloj]

The LP-DED process can form near-net shape blanks, final-shape components, and integral features within components providing the ability to significantly reduce part count. The advantages of the process are numerous, with the main application being significantly larger scale and higher deposition rates than L-PBF, and the ability to use multiple materials and functional gradient material deposition strategies [10,11,12]. Through adapting the deposition heads to multi-axis robots and gantry systems, features can be added locally on parts creating near net or near-final shape significantly reducing the need for support structures or added stock. The material is deposited in a local purge or a fully inert environment to minimize oxidation. These aspects of the LP-DED technology allow for large, complex

curvature component shapes to be created with multiple ports or non-symmetric features. This includes internal features, pockets or structures, such as coolant channels in nozzles or other heat exchanger components [13].

While there are several advantages of the process, it has some challenges compared with the L-PBF process. The laser focus and subsequent melt pool size, which is controlled with the spot size and key parameters, is much larger than L-PBF. Various spot sizes, and subsequent melt pool size, can be adjusted or tailored to the component features being deposited. The key parameters used in the process include laser power, travel speed, powder feedrate, layer height, and stepover. The parameters establish the melt pool and resulting bead width being deposited and the features that are achievable with a particular parameter set and corresponding spot size. The powder size is typically 45-105 $\mu\text{m}$ , but can also be reduced to 15-45  $\mu\text{m}$  to allow for reduced surface roughness.

The features that can be deposited using LP-DED are also much larger than L-PBF. LP-DED offers a good trade between high deposition rates --which allows for much higher build rate than L-PBF—and resolution of features [14]. The trade of the higher deposition rate is loss of resolution in features such as small holes, channels, wall thicknesses. These spot sizes, and subsequent melt pool, can be adjusted or tailored to the component features being deposited. The minimum wall thicknesses most common in DED are 0.04" (1 mm) [15,16]. While thinner walls have been created successfully, there are additional design and build restrictions on these walls. The walls are required to have more support features so they do not self-collapse, and deposition rates will be significantly reduced. LP-DED results in a coarser wall with waviness in addition to an overall rougher surface finish than the powder bed technology. Because of the impact of surface finish on fatigue life and flow performance, post-processing may be required with DED [17,18,19].

The LP-DED process provides an overall advantage to fabricate large scale hardware (>5 feet diameter and >7 feet height) while still maintaining thin-walls (0.040 inches / 1 mm). This requirement is focused on the application of regeneratively-cooled nozzles to reduce the fabrication time and allow for a fully integral channel wall nozzle built with only a few parts. While the process was being developed to achieve these features, the development of an enabling alloy was also initiated.

## **B. Overview and Development of the NASA HR-1 Alloy**

NASA HR-1 is a high-strength Fe-Ni superalloy designed to resist high pressure, hydrogen environment embrittlement, oxidation, and corrosion. NASA HR-1 was originally developed at NASA in the 1990's and derived from JBK-75 to increase strength and ductility in high-pressure hydrogen environments. The NASA HR-1 chemistry was formulated to meet requirements for liquid rocket engine (LRE) applications, specifically components used in a high-pressure hydrogen environment. LRE components provide extreme and challenging environments for materials throughout engine operation. Component structures used in LREs can require very thin walls, in regeneratively-cooled nozzles for instance, that provide challenges with thermal and structural loads. Additionally, combining the environment with liquid and gaseous hydrogen propellant to the thermal and structural loads provides an even more complex challenge. For these applications, materials must be designed to resist Hydrogen Environment Embrittlement (HEE). Furthermore, these components have key requirements to consider for materials selection, including thermal conductivity, low cycle fatigue (LCF), yield strength, and elongation.

While a few materials are available to meet these requirements, there are trades that must be made amongst the various properties during operation, which could make the design heavier than necessary or lead to premature failure due to low margins. Aerospace structural alloys that encounter gaseous hydrogen in operation (for example, hot gas manifolds in a rocket engine and hot-wall of a rocket nozzle) require adequate resistance to HEE in addition to good strength and oxidation/ corrosion resistance. Austenitic stainless steels, A-286 and JBK-75 are commonly used in such applications. However, these alloys have their limitations. Austenitic stainless steels (such as 304, 310, and 316) are hydrogen-resistant, but have low yield strength (around 276 MPa). Fe-base superalloys that are derived from austenitic stainless steels (such as A-286, and JBK-75) have adequate resistance to HEE, corrosion, and oxidation, but lack high strength. In consideration of these problems, NASA HR-1 was specifically developed as a higher strength structural alloy that has combined virtues of HEE, oxidation, and corrosion resistance [20].

When NASA HR-1 was being designed, it was evident that hydrogen-resistant Fe-base superalloys, such as A-286, JBK-75, have  $\gamma$ -matrix compositions evolving from hydrogen-resistant stainless steels (single  $\gamma$ -phase materials) [21]. The alloy development was approached by formulating a hydrogen-resistant  $\gamma$ -matrix that resembles JBK-75 along with increasing  $\gamma'$  volume fraction and strengthening  $\gamma$ -matrix. The matrix phase,  $\gamma$ , is a solid solution of Fe, Ni, Co, Cr, Mo, W, and V. Whereas the precipitate phase  $\gamma'$  is composed of hardening elements Ti and Al. Another precipitate phase was observed in the microstructure, the  $\eta$ -phase. This  $\eta$ -phase is a Ti-rich acicular precipitate that forms along grain boundaries under certain heat-treated conditions, and it forms within the grains after prolonged exposure to elevated temperatures.

#### IV. NASA HR-1 Alloy Chemistry Optimization

There are five key requirements to consider for LRE nozzle material selection, including yield strength, thermal conductivity, HEE resistance, ductility, and low cycle fatigue (LCF). These five material properties are all interrelated and must be taken into consideration when optimizing the formulation and heat treatment for LP-DED NASA HR-1. After conducting a methodical assessment, it was determined that the most appropriate way to obtain an optimal compromise of these five materials properties is through a moderate strength reduction as shown in Figure 2. A moderate 10 - 15% strength reduction is expected to increase ductility, LCF life, and maintain good HEE resistance and thermal conductivity. To date, an optimal compromise of these five important properties has been accomplished through optimization of alloy chemistry and heat treatment.

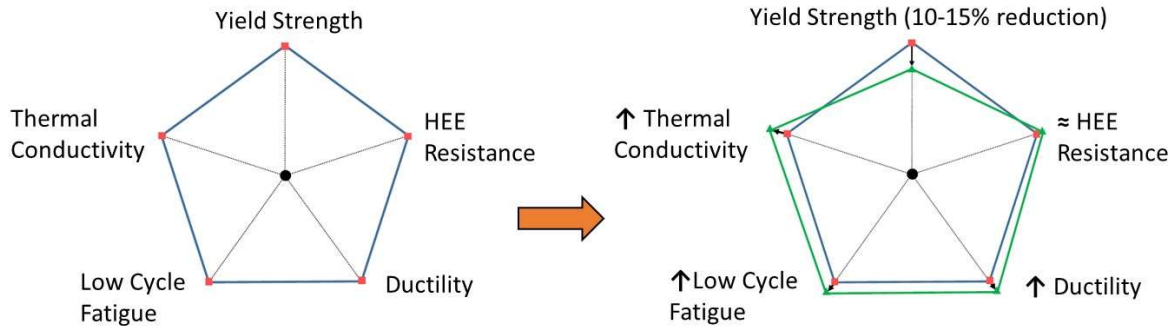


**Figure 2. Material design criteria and key trades to optimizing for a nozzle application. This shows the transition of the original NASA HR-1 formulation to the Rev. 3 formulation.**

During the early stage of LP-DED NASA HR-1 development, it was discovered that the DED process promotes titanium segregation and grain boundary  $\eta$ -phase precipitation more than the conventional wrought process [22]. Therefore, the chemical composition of wrought NASA-HR1 was modified using the PHACOMP method [23, 24, 25, 26] to make NASA HR-1 more suitable for additive manufacturing.

Based on the PHACOMP approach, an optimal composition of NASA HR-1 (Rev 3) was formulated [27]. Table 1 shows the chemical composition of NASA HR-1, A-286, and JBK-75. AM NASA HR-1 Rev 2 and Rev3 represent the 2<sup>nd</sup> and 3<sup>rd</sup> composition modifications that were made by the PHACOMP method.

**Table 1. Nominal Chemical composition (wt%) for NASA HR-1.**

Alloy	Fe	Ni	Cr	Mo	V	W	Co	Ti	Al	Mn
Wrought NASA HR-1	38.90	34.10	15.50	2.40	0.30	2.20	3.50	2.80	0.30	-
AM NASA HR-1 Rev 2	39.80	34.00	15.50	2.20	0.32	2.10	3.30	2.50	0.25	-
AM NASA HR-1 Rev 3	41.20	34.00	14.60	1.80	0.30	1.60	3.80	2.40	0.25	-
Wrought A-286	55.20	25.00	15.00	1.30	0.20	-	-	2.00	-	1.50
Wrought JBK-75	51.13	30.20	14.75	1.25	0.30	-	-	2.10	0.25	-

NASA HR-1 Rev 3 is the latest optimized composition that is specially formulated to obtain an optimal compromise of five key material properties for LRE nozzle application. The reduction of Ti content is expected to retard grain boundary  $\eta$ -phase precipitation and improve ductility and LCF performance.

#### C. Heat Treatment Development

The as-deposited LP-DED NASA HR-1 has a high degree of titanium segregation in the interdendritic regions [22]. Titanium segregation promotes precipitation of  $\eta$ -phase at grain boundaries that is detrimental to tensile ductility, LCF life, and resistance to hydrogen environment embrittlement. Therefore, an improved post-processing heat treatment was developed to mitigate titanium segregation and  $\eta$ -phase precipitation for LP-DED NASA HR-1. A heat treatment development plan was put together based on the homogenization kinetic analysis [22] as shown in Table 3..

A higher temperature stress relief at 1950 °F was attempted to see the effects of stress relief temperature on grain structure evolution. Homogenization treatment was extended for times up to 12 hours at 2125 °F. It is a great concern that the standard solution anneal temperature of 1800 °F is too close to the  $\eta$ -phase solvus temperature according to the  $\eta$ -phase TTP diagram [28]. Therefore, higher temperature solution anneal at 1950 °F was also attempted to ensure  $\eta$ -phase is completely dissolved and Ti concentration at grain boundary is kept at a low level prior to the final aging treatment.

**Table 2. Heat treatment development plan for LP-DED NASA HR-1.**

	Stress relief (°F/hrs)			Homogenization (°F/hrs)			Solution anneal (°F/hrs)		
	1800/1.5	1950/1.5	1950/3	2125/3	2125/6	2125/12	1800/1	1950/1	1950/3
Standard heat treatment	√			√			√		
Heat treatment development		√	√		√	√		√	√

#### D. Effects of stress relief on grain structure evolution

Stress relief treatment is intended to relieve the internal strain energy and must be performed at a high enough temperature to activate the recovery process. Recrystallization during stress relief is desirable for LP-DED NASA HR-1 to transform the as-built coarse columnar dendritic microstructure to finer and more equiaxed grain structure. Effects of stress relief temperature on microstructure evolution for single-pass LP-DED NASA HR-1 samples (3.175 mm thick) are presented in Figure 3. As shown, the sample that received stress relief at 1700 °F exhibits dominant dendritic structure, indicating 1700 °F is well below the recrystallization temperature. Significant microstructure evolution occurred when the stress relief temperature is above 1800 °F. Due to partial recrystallization, the as-built dendritic structure had transformed to heterogeneous grain structure after stress relief at 1800 and 1900 °F for 1.5 hours.

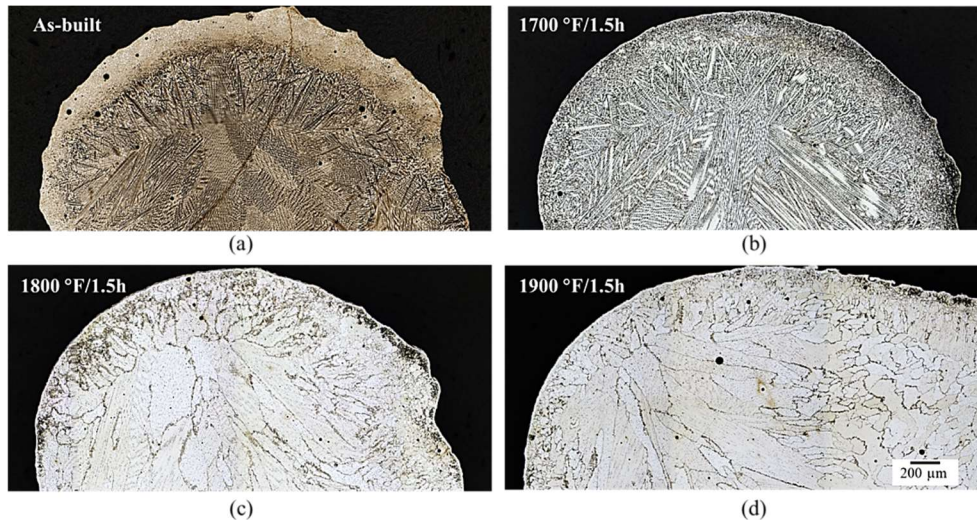


**Figure 3. Effects of stress relief on microstructure evolution for LP-DED NASA HR-1. The stress relief conditions are (a) as-built, (b) 1700 °F/1.5h, (c) 1800 °F/1.5h, and (d) 1900 °F/1.5h.**

After stress relief, varying degree of recrystallization occurred when the material was HIPed. As shown in Figure 4, the grain structure evolution after HIP is sensitive to the stress relief temperature. The grain structure is finest for the samples that received stress relief treatment at 1900 °F/1.5h. It is apparent that higher stress relief temperature prior to HIP promotes recrystallization and decreases grain size. Similar grain size reduction was accomplished when LP-DED NASA HR-1 was stress relieved at 1950 °F/1.5h and followed by a homogenization treatment at 2125 F°/3h [29]. One of the most important effects of post-processing heat treatment for AM materials is microstructure

refinement. It is desirable to have finer and more equiaxed grain structure. Therefore, 1950 °F/1.5h was chosen to be the new stress relief treatment for LP-DED NASA HR-1.

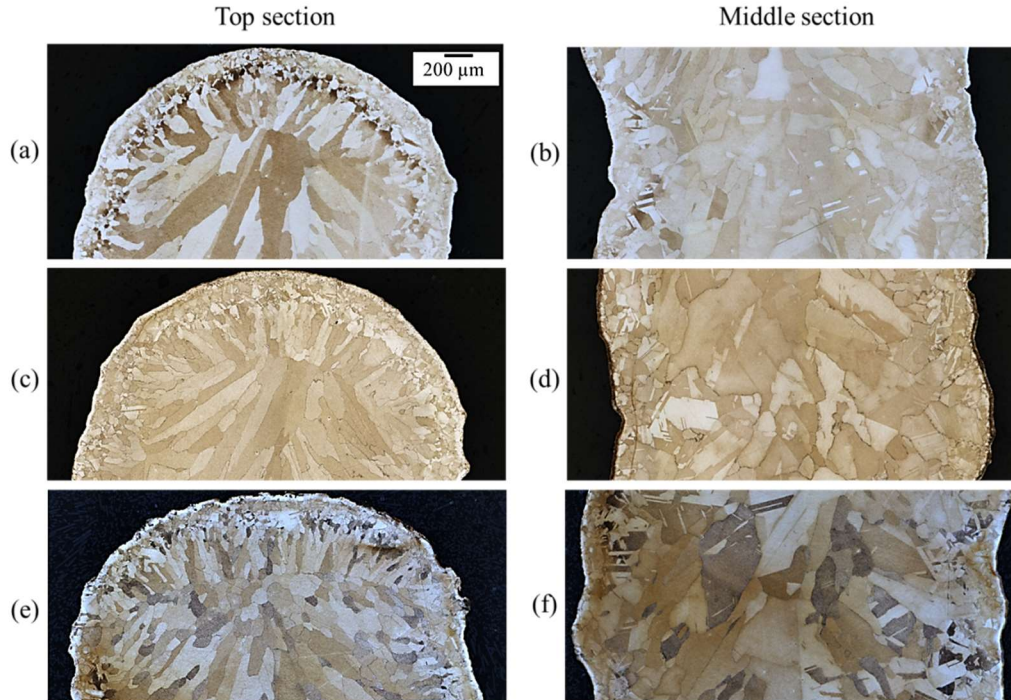


**Figure 4. Microstructure evolution of LP-DED NASA HR-1 samples that received stress relief treatment for 1.5 hours at (a) and (b) 1700 °F, (c) and (d) 1800 °F, and (e) and (f) 1900 °F followed by HIP.**

#### **E. Reduction of Ti segregation through homogenization treatment**

Evolution of titanium segregation in LP-DED NASA HR-1 before and after post-processing homogenization has been investigated in detail [22]. A basic model for titanium diffusion in NASA HR-1 was developed to project concentration distribution of titanium as a function of homogenization temperature, duration, and grain size. The results of the homogenization kinetic analysis provide a valuable reference on how the homogenization treatment should be adjusted for LP-DED NASA HR-1. Titanium distribution was determined by Energy Dispersive Spectroscopy (EDS) line scans. The as-deposited LP-DED NASA HR-1 has a high degree of titanium segregation. Titanium concentration fluctuated intensely between 0.3 to 6% in many locations.

Ti segregation can be greatly reduced after homogenization at 2125 °F. The fluctuation of Ti concentration amplitude was reduced from 0.3 - 8% (in the as-built condition) to approximately 1.0 - 4.5% after homogenization at 2125 °F/3h. But Ti concentration is still significantly higher than the nominal 2.5 wt% in many locations. An increase of the homogenization time to 6 hours leads to noticeable improvement in Ti segregation as shown in Figure 7 (b). After homogenization at 2125 °F/6h, titanium segregation amplitude decreased and most Ti peaks fluctuated in the range of 1.0 - 3.5%. However, further increase of the homogenization time to 12 hours leads to only marginal improvement in Ti segregation amplitude.

The EDS line scan results indicated the current homogenization treatment at 2125 °F/3h is not adequate to reduce titanium segregation to an acceptable level for LP-DED NASA HR-1. Due to the coarse grain structure in LP-DED NASA HR-1, higher homogenization temperature or longer duration should be performed in order to reduce Ti segregation to a very low level [22]. However, the use of a temperature higher than 2125 °F is not recommended due to the increased risks of surface oxidation, grain growth and potential growth of internal pores. Performing a homogenization treatment at 2125 °F for duration longer than 12 hours cannot be justified either as reduction of Ti segregation becomes very sluggish after the initial 6 hours at 2125 °F. Therefore, 2125 °F/6h is selected to be the new homogenization treatment for LP-DED NASA HR-1.

### F. Mitigation of $\eta$ -phase precipitation through solution anneal and aging treatment

After homogenization, solution anneal and aging processes are performed sequentially to precipitate and grow the strengthening  $\gamma'$  precipitate ( $\text{Ni}_3(\text{Ti},\text{Al})$ ). The solution anneal temperature should be above the  $\eta$ -phase solvus temperature and the time should be long enough to dissolve  $\eta$ -phase. The standard solution anneal for LP-DED NASA HR-1 is 1800 °F/1h, which is only approximately 50 °F above the  $\eta$ -phase solvus temperature [29]. Therefore, solution anneal temperature was increased to 1950 °F to ensure complete dissolution of  $\eta$ -phase.

The standard aging treatment for wrought NASA HR-1 is 1325 °F/16h. It was discovered that the standard 1325 °F/16h aging treatment was unable to reduce the brittle  $\eta$ -phase to an acceptable level for LP-DED NASA HR-1, primarily due to high magnitude of Ti segregation. Therefore, the aging temperature must be lowered to 1300 °F or 1275 °F in order to mitigate  $\eta$ -phase precipitation. Figure 5 shows grain-boundary  $\eta$ -phase precipitation when aging treatment was performed at 1325 °F, 1300 °F, and 1275 °F. Grain boundaries are  $\eta$ -phase free after solution anneal at 1800 °F/1h as shown in Figure 8 (a). Abundant  $\eta$ -phase precipitated at grain boundaries after aging at 1325 °F/24h. The volume fraction of grain-boundary  $\eta$ -phase decreases significantly when the aging temperature was lowered to 1300 °F (Figure 5 (c)). Only a few isolated  $\eta$ -phase indications were present at grain boundaries after aging at 1275 °F/16h (Figure 5 (d)). It is apparent that the amount of grain-boundary  $\eta$ -phase decreases with a reduction in aging temperature. Therefore, 1275 °F was selected as the 1<sup>st</sup> step aging temperature.

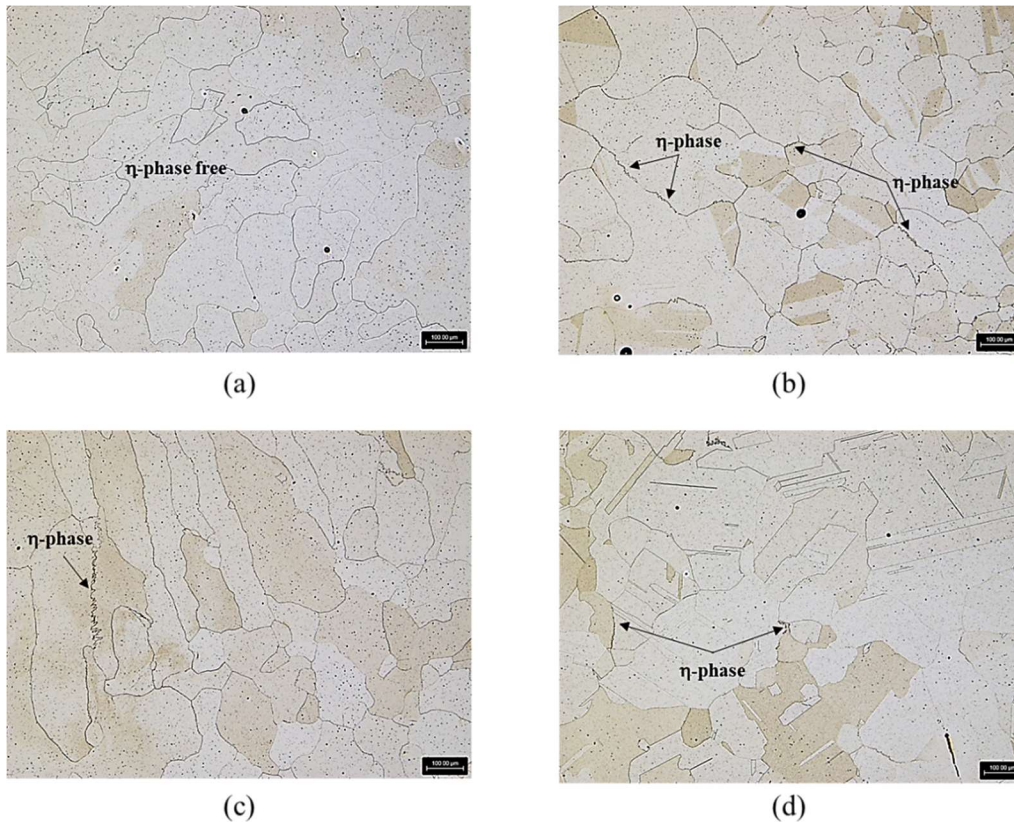


**Figure 5. Grain-boundary  $\eta$ -phase precipitation after (a) solution anneal, (b) aging at 1325 °F/24h, (c) aging at 1300 °F/24h, and (d) aging at 1275 °F/16h.**

Lowering the aging temperature to 1275 °F is expected to result in a significant reduction in tensile strength. In order to keep the strength reduction within a moderate 5 - 15% range, the standard single-step aging treatment must be modified into a 2-step aging process. Therefore, 1200 °F and 1150 °F were selected as the 2<sup>nd</sup> step aging temperatures with a soak time of 16 hours. The most promising 2-step aging treatment would be chosen after performing an in-depth analysis on tensile data, which includes yield strength, ultimate tensile strength, ductility, and strain hardening exponent  $n$  ( $\sigma = k\epsilon^n$ ). Four aging treatments were selected for tensile property evaluation as shown

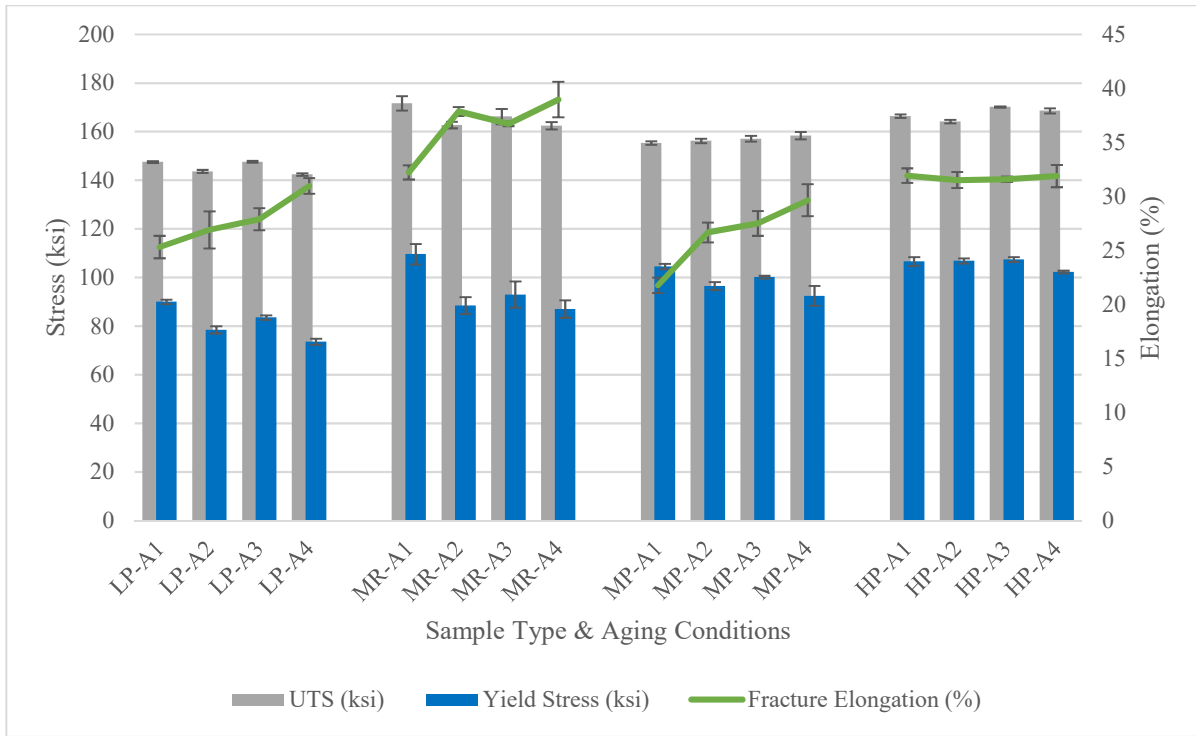
in Figure 9. The standard aging treatment for wrought NASA HR-1, 1325 °F/16 h, was included as the baseline for comparison with the other three aging treatments.

### **G. Effects of Heat Treatments on Mechanical Properties**

To examine the impacts of heat treatments and deposition parameters on mechanical properties, monotonic tensile tests were performed at NASA MSFC using LP-DED NASA HR-1 samples built with three different deposition parameters that could be used to produce parts. All tests were performed in air at room temperature with the as-deposited wall thickness and surface finish for single pass plates labeled in Figure 6 as LP and MP, while MR and HP were fully machined rounds and plates with thicknesses of approximately 0.35” and 0.25”, respectively. All samples were subjected to the same stress relief, homogenization, and solution anneal as the standard heat treatment in table 3, and from each deposition parameter, there were sets of samples subjected to one of four different aging cycles mentioned previously and shown in Figure 6.

Figure 9 shows the average strengths and fracture elongation for LP-DED NASA HR-1 tensile testing samples described previously. In general, it was observed that the ductility increased from the A1 to A4 conditions while yield strengths expectedly decreased. These trends are observed due to a reduction in  $\gamma'$  content in the material caused by the reduced temperatures of the aging cycles. Slight variations in ultimate tensile strength (UTS) were observed between aging conditions, however the only significant difference was in the medium deposition rate round bars with the A1 aging condition. The variations observed between the different sample types can be attributed to the difference in sample cross sectional area of the plates and round bars.

While the same general trends in UTS, yield strength, and elongation were observed for the low and medium deposition rate samples, the high deposition rate plates did not appear to be impacted by the differences in aging cycles. The high deposition rate microstructure had not been examined prior to testing, so further investigation was needed. Upon examination of the microstructure, these samples were observed to have areas of very large grains ( $>500 \mu\text{m}$  or 0.020”) and areas of finer grains ( $<250 \mu\text{m}$  or 0.010”) shown in Figure 7. This bimodal behavior is due to the build strategy of the parts during the DED process as layers overlap in different directions and grain growth competes in different directions.



LP	Low Deposition Rate Plate (350W 0.047" T)	A1	1325 F/16h
MR	Medium Deposition Rate Round Bar (1070W)	A2	1300 F/16h
MP	Medium Deposition Rate Plate (1070W 0.140" T)	A3	1275 F/16h + 1200 F/16h
HP	High Deposition Rate Plate (2620W 0.25"T)	A4	1275 F/16h + 1150 F/16h

**Figure 6. Average test results of room temperature monotonic tensile testing of various LP-DED NASA HR-1 samples that had been subjected to the same stress relief, homogenization, and solution anneal then treated with different aging cycles to examine the impacts.**

In comparison, the low and medium deposition plates were observed to have much finer grains and a more uniform grain structure. These plates were also deposited with single passes parallel to each other which resulted in some directional grains, however these instances are limited. The set of samples used for testing were also observed to have a slightly finer grain structure in the low deposition rate (Figure 7 bottom left) and a much finer grain structure in the medium deposition rate (Figure 7 bottom right) than previous samples examined (Figure 4 and [30]). This finer grain structure has been attributed largely to the compositional change from revision 2 to revision 3.

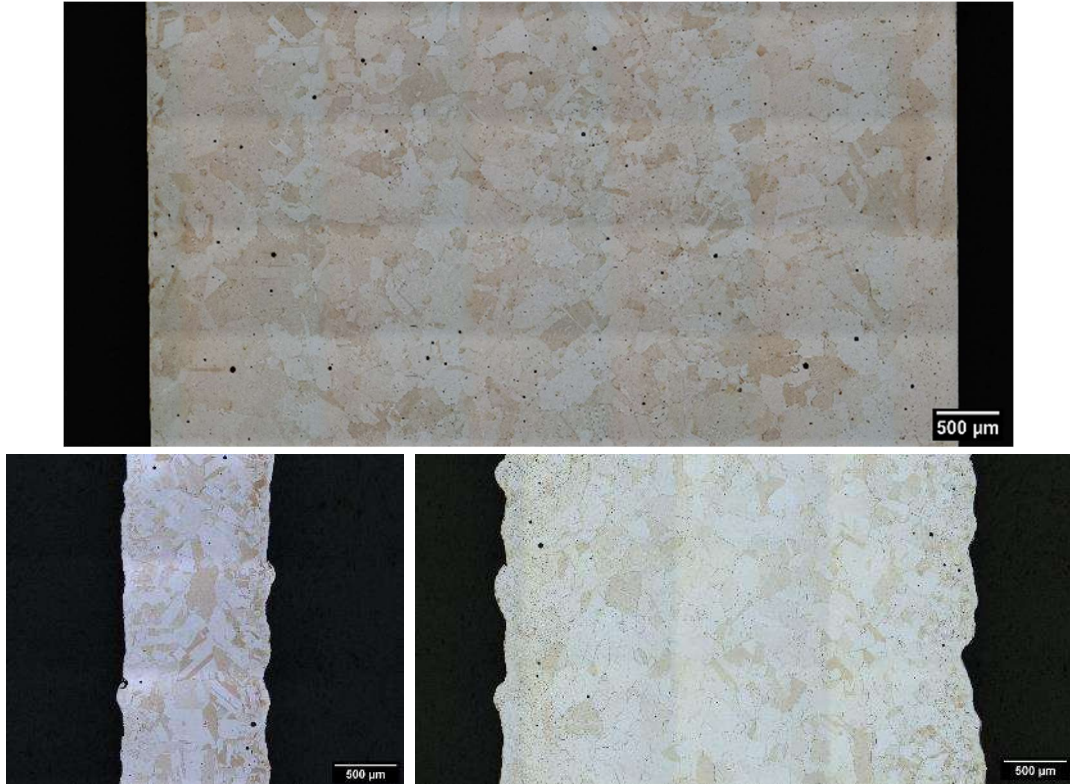


**Figure 7. Optical micrographs of etched grain structure of LP-DED NASA HR-1 after heat treatment.**  
*Top: 2620W Plate; Bottom Left: 350W Plate; Bottom Right: 1070W Plate*

Table 3 summarizes the effects of aging treatment on room temperature tensile properties for LP-DED NASA HR-1 1070W round bars and 350W plates. The 1070W - 0.339" diameter round bar samples have an average yield strength, ultimate tensile strength, and fracture elongation of 87.02 - 109.60 ksi, 162.40 - 171.61 ksi, and 32.23 - 38.97%. The 350W - 0.047" thick samples have an average yield strength, ultimate tensile strength, and fracture elongation of 73.57 - 89.58 ksi, 142.37 - 147.61 ksi, and 25.32 - 30.97%. The 0.047" thick single-pass samples, which have very large grain size, display excellent strain hardening exponent that are critical for LRE nozzle application. It is encouraging to note that NASA HR-1 is suitable for fabricating very thin panels using the DED method as the 350W 0.047" thick samples are very ductile and have excellent strain hardening capability. One 1070W - 0.339" diameter round bar sample that has the highest tensile strength was selected from each aging treatment to compare the strain hardening behavior. Signs of high strain hardening capability are delayed necking, high elongation, and lower yield strength. As shown in Figure 7, it is apparent that A4 2-step aging treatment, 1275 °F/16h + 1150 °F/16h, yields higher strain hardening capability than the others.

**Table 3. Effects of aging treatment on tensile properties for LP-DED NASA HR-1.**

Laser Power & Sample Configuration	Aging Treatment	Aging Treatment	Yield Stress (ksi)	Tensile Stress (ksi)	Fracture Elongation (%)	Strain hardening exponent (n)	n ranking
350 W 0.248" W x ~0.047" T	1325 F/16h	1	89.98	147.52	25.32	0.210	4
	1300 F/16h	2	78.48	143.62	26.91	0.250	2
	1275 F/16h + 1200 F/16h	3	83.54	147.61	27.89	0.237	3
	1275 F/16h + 1150 F/16h	4	73.57	142.37	30.97	0.274	1
1070 W Round bar (0.339" diameter)	1325 F/16h	1	109.60	171.61	32.23	0.198	4
	1300 F/16h	2	88.44	162.74	37.87	0.263	2
	1275 F/16h + 1200 F/16h	3	92.95	166.19	36.74	0.251	3
	1275 F/16h + 1150 F/16h	4	87.02	162.40	38.97	0.271	1

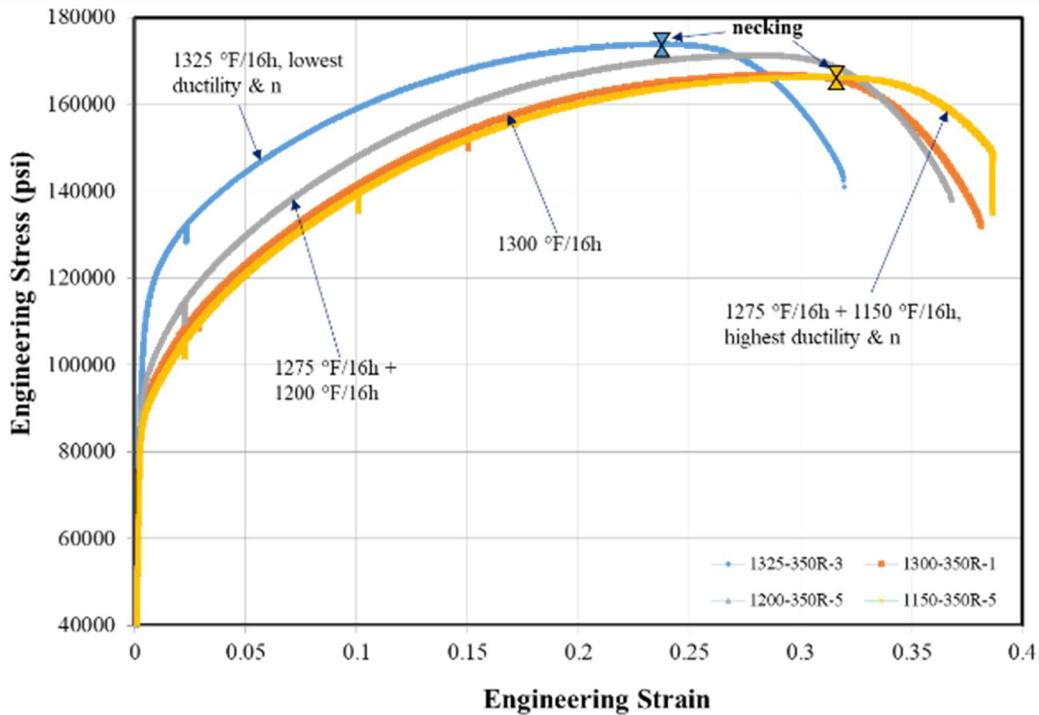


**Figure 8. Overlaid stress-strain curves for the sample that has the highest tensile strength from each aging treatment group.**

One key takeaway from the tensile data analysis is A4 2-step aging treatment yields significantly higher tensile ductility and strain hardening exponent than the standard single-step aging treatment (1325 °F/16h). The strain hardening exponent ranking is A4 > A2 > A3 > A1. The material that has high strain hardening exponent can store more strain energy, diffuse deformation, and improve LCF performance. Strain hardening behavior is microstructure dependent and the improved strain hardening capability can be attributed to the presence of finer and underaged  $\gamma'$  precipitate. Therefore, A4 (1275 °F/16h + 1150 °F/16h) is the most promising and has been selected as the new aging treatment for LP-DED NASA HR-1. The evolution of post-processing heat treatment for LP-DED NASA HR-1 from the early stage heat treatment to the new heat treatment is given in Figure 9.

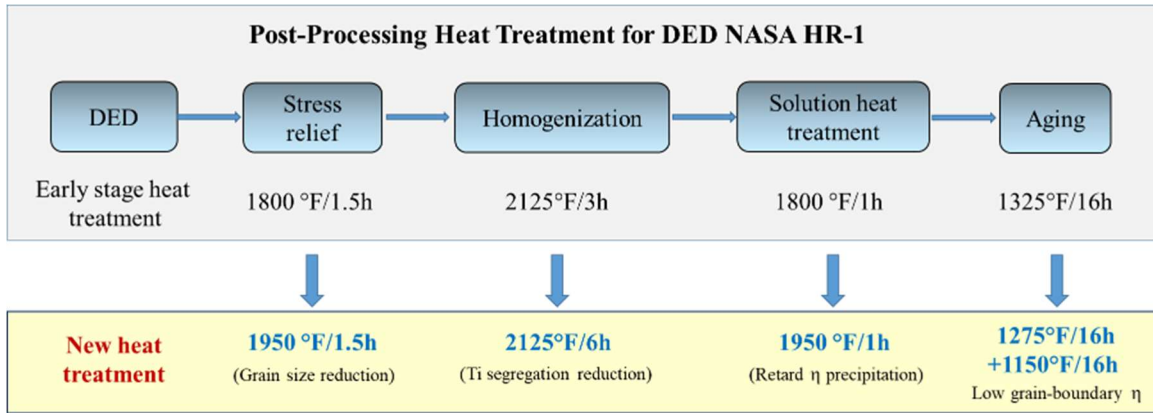


**Figure 9. The evolution of post-processing heat treatment for LP-DED NASA HR-1.**

After analysis of the tensile properties, preliminary low cycle fatigue tests were performed at 1% total strain  $R=-1$  and room temperature in air to get a bearing on the fatigue performance of LP-DED NASA HR-1 using the standard stress relief, homogenization, and solution treatment followed by the two step aging cycles A3 and A4. From this preliminary testing, there was not a significant difference in cycles to failure between the two different aging cycles with both sets exceeding 6500 cycles for the lowest point. As further testing is completed examining higher strains, the material’s fatigue behavior can be fully characterized. When compared to wrought NASA HR-1 tested in high pressure GHe shown in Figure 10, the DED material had a reduction in the cycles to failure which is likely due to the difference in microstructure between the DED material and wrought. The difference between wrought and LP-DED NASA HR-1 is further illustrated Figure 10 with the tensile testing properties for round bar specimens in air. A drop in strength in the DED material was expected due to the microstructure and adjustments in heat treatment for the A4 aging cycle, however a significant increase in ductility was also noted.

In summary, LP-DED NASA HR-1 exhibits expected trends in strength and ductility as temperatures of aging cycles are reduced. Changes from the standard single step aging cycle to a lower temperature two step aging cycle resulted in improved strain hardening behavior that is important for low cycle fatigue environments like those in LRE components. The tensile properties and the low cycle fatigue properties of LP-DED NASA HR-1 were observed to be lower than the wrought material with the standard heat treatment being used and with adjusted aging cycles. This drop is part of the trade when using additive manufacturing, and is thus expected. Further adjustments in the heat treatment cycles have been proposed to improve upon the issue of Ti segregation observed in LP-DED NASA HR-1 and mechanical testing to characterize these new heat treatment cycles are planned.

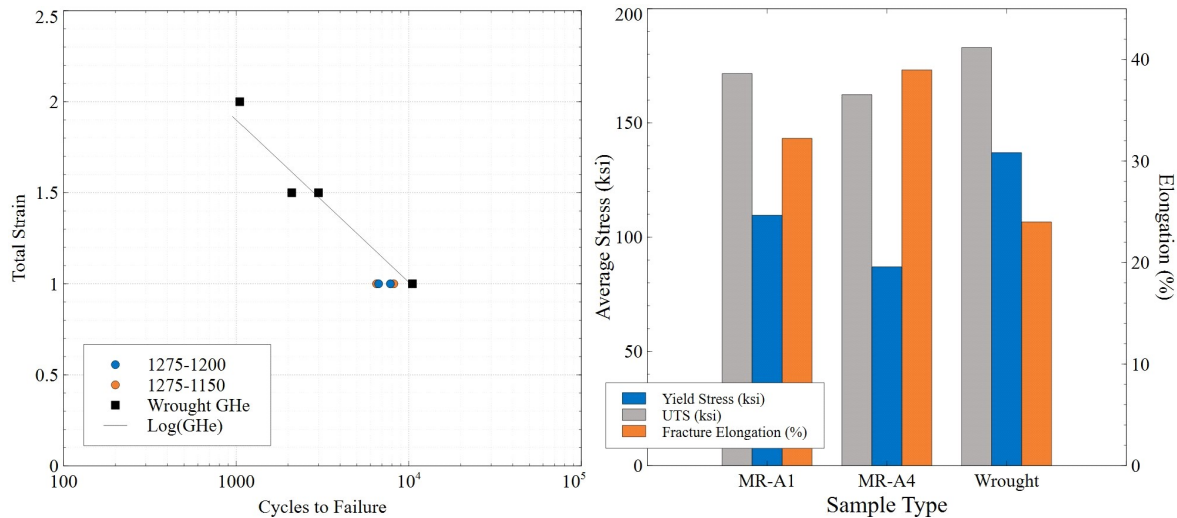


**Figure 10. Comparisons of mechanical testing results of LP-DED NASA HR-1 to wrought NASA HR-1. Left: Low cycle fatigue testing; Right: Monotonic tensile testing. Wrought data plotted from [31]**

## V. Demonstration Hardware using LP-DED NASA HR-1

While material characterization, heat treatment development and characterization were ongoing, the process required further advancements to understand the build limitations and the general design rules for the process. Some of these initial design rules for the LP-DED process were highlighted in [32]. One advantage of the LP-DED process is the ability to tailor the deposition rate based on the wall thickness of the part using various spot sizes and changes in parameters. Several parts were fabricated using various sets of deposition parameters and spot sizes. This section will highlight some of the hardware process development.

### A. Injector/Powerhead Hardware

The main focus of the LP-DED process has been for integral channel wall nozzles, but several other components were fabricated that had potential advantages using this alloy. These parts included manifolds for fluid distribution of channel wall nozzles and other components, powerhead housing and liners, and fluid transfer ducts used in a hydrogen environment. While the channel wall nozzle uses a low deposition rate ( $<1$  in<sup>3</sup>/hour) to allow for the fine features, many of these parts (shown in Figure 11) used a much higher deposition (3-5 in<sup>3</sup>/hour) rate since the designs were thicker wall and did not require internal complex features, such as channels. These designs were evaluated as a forging or casting replacement that allows further reduction of machining time. In Figure 11A, a liner is shown with uniform wall thickness, but non-symmetric ports. Similar hardware is shown in Figure 11B with a constant wall manifold at 0.2" with an integral inlet port. Figure 11C and Figure 11D shows demonstrator parts for the RS-25 powerhead that includes the hot gas manifold oxidizer and fuel shells, respectively. Each of these parts were deposited in less than 14 days with a high deposition rate.



**Figure 11. Examples of thick-wall LP-DED hardware. A) Liner for powerhead, B) 24" dia. manifold for subscale nozzle, c) RS-25 hot gas manifold oxidizer shell, D) RS-25 hot gas manifold fuel shell.**

### B. Channel Wall Nozzle Development Hardware

A majority of the process development was focused on hardware supporting channel wall nozzles to determine design constraints and options for further development. NASA previously reported the fabrication of an integral channel LP-DED nozzle that was 40" diameter and 38" height that was successfully fabricated in 30 days [33]. This demonstrator unit was successfully built with powder removed from the channels and minimal distortions ( $<0.02$  inches / 0.51 mm) from the nominal design. Based on this success, a larger scale demonstrator was designed using the process that would maximize the current machine capabilities. The nozzle was produced on a RPM Innovations (RPMI) 557, which provides a build envelop of 5 x 5 x 7 feet (1.52 x 1.52 x 2.13 meters). This nozzle, as with all

designed using LP-DED incorporate a constant hot-wall and channel lands. This large demonstrator, titled the 65% scale manufacturing technology demonstrator (MTD), was representative of a 65% RS-25 nozzle. The 65% MTD can be seen in Figure 12.

The diameter was 58 inches (1.47 meters) and the total height was 72 inches (1.83 meters) with fully integral channels, and the part was built in 90 days. The 65% MTD was designed as a 1.8-pass nozzle with coolant entering at the forward end channel down-pass toward the aft end, turning around at the aft end, and channel up-pass exiting as shown. With a constant channel land/rib thickness, the channels continuously varied on the width. The nozzle was built with the bell end up and pre-planned stops were determined to remove excess powder from the build chamber and visual inspections. The trunnion (tilt) table was also angled in a few discrete positions as the height increased in an attempt to keep the deposition head approximately normal to the nozzle wall.



**Figure 12. NASA HR-1 65% scale integrated channel wall nozzle fabrication using LP-DED built in 90 days [Diameter = 58 inches (1.47 meters) and the total height was 72 inches (1.83 meters)].**

A series of other nozzles have completed LP-DED fabrication that include 1.2K-lb<sub>f</sub>, 7K- lb<sub>f</sub>, and 40K- lb<sub>f</sub> scale for hotfire testing. These nozzles all used a similar design strategy with a constant hot-wall and channel land thickness to aid with the deposition process. The hot-walls were reduced using a chemical mechanical polishing (CMP) process. These nozzles are all designed with a bifurcation as the diameter increases on the nozzle to maintain a pre-described width to avoid a large span in the channel and potential structural failure. An example of the 40K- lb<sub>f</sub> nozzle and a CMP processed nozzle is shown in Figure 13. The 40K-lbf nozzle was designed and deposited with square channels but a spiral pattern axially to distribute any local heat load (streaking) across multiple channels. The 1.2K- lb<sub>f</sub> nozzle shown in the image incorporated straight-pass channels.

One unique configuration that was demonstrated was to replicate a tube-wall structure. The channels were D-shaped with a scalloped hot-wall, but also spiraled as shown in Figure 14. The channel land was constant, but the radius on the scalloped hot-wall varied based on the width of the channel. The CMP process was also used to reduce the hot-wall and achieved a high degree of polishing even within the region between the scallops.



**Figure 13. NASA HR-1 Nozzles fabricated using LP-DED process. (Left) 40K- lb<sub>f</sub> nozzle with spiral channels with manifolds fitted prior to EB welding, (Right) 1.2K- lb<sub>f</sub> nozzle hot-wall after CMP processing.**



**Figure 14. 1.2K- lb<sub>f</sub> integral channel LP-DED scalloped spiral nozzle hot-wall after CMP processing.**

## VI. Hot-fire Testing Summary

To further mature the LP-DED technology with NASA HR-1, several nozzles were designed and fabricated. This section will specifically highlight a 7K- lb<sub>f</sub> nozzle development and hot-fire testing and also 2K- lb<sub>f</sub> hardware with testing ongoing as of this publication. The program, titled Long Life Additively Manufactured Assembly (LLAMA), was developed in an effort to demonstrate high duty cycle performance comparable to that of traditionally manufactured thrust chamber assemblies (TCA) and incorporated a bolted NASA HR-1 LP-DED nozzle. All LLAMA hardware was tested under NASA test series PK058 and PK129 at NASA Marshall Space Flight Center (MSFC) in the east test area at test stand 115 (TS115). The propellants were Liquid Oxygen/Methane (LOX/CH<sub>4</sub>) with steady-state chamber pressures above 650 psig and mixture ratio (MR) from 2.65 to 3.19. The objective of this test campaign was to subject the LLAMA chamber to a minimum of 50 hot-fire cycles at thermal steady state conditions to assess the hardware's lifecycle performance. The hardware configuration included a GRCop-42 L-PBF chamber, L-PBF impinging injectors and the nozzle. This section will discuss the fabrication of the nozzle, hot-fire testing campaign and results.

The 7K- lb<sub>f</sub> nozzle was designed similar to the prior nozzles described with a constant channel land and hot-wall deposited using NASA HR-1 alloy. The channels were also variable width and had a smooth hot-wall design with

straight axial channels. The nozzle was deposited with the bell-end up for a majority of the liner and channels. The nozzle was then rotated using the tilt on the trunnion table to deposit the manifold weld preparations. This allows for the design to eliminate support structures or stock material and minimize machining. The nozzle was deposited in approximately 11 days. Following LP-DED, any excess powder was removed and the part was bead blasted on the external surfaces only. A laser scan was then completed of the nozzle and showed minimal distortion from the deposition process that would allow machining to the drawing as expected. The nozzle completed a stress relief, homogenization, and solution heat treatments. After heat treatments in the annealed condition, the manifold weld preparations on the nozzle were machined along with the mating manifolds. The forward and aft manifolds were machined from 304L forgings. The forward manifold manifold was designed for an electron beam (EB) weld while the aft manifold was manually Gas Tungsten Arc Welded (GTAW) or Tungsten Inert Gas (TIG). The nozzle and manifolds completed cleaning operations prior to welding of the manifolds. The general deposition process is shown in Figure 15.

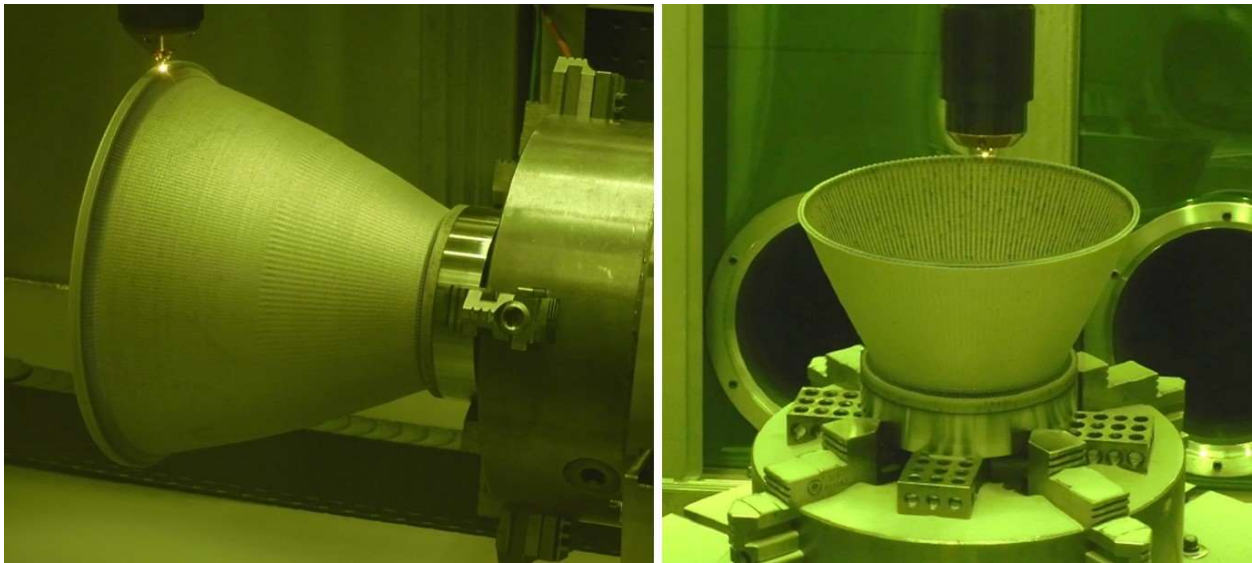


**Figure 15. Laser powder directed energy deposition (LP-DED) for the LLAMA 7k nozzle.**

Following welding of the manifolds, the nozzle was sent to a vendor for CMP processing. Following CMP, the forward interface of the nozzle was final machined and the inlet tubes and ports were welded, and the outlet ports were installed. The nozzle was also designed with integral pressure and temperature instrumentation ports in manifolds. Finally, the nozzle was aged, inspected, and proof tested. The nozzle successfully completed proof with no leakage observed. A visualization of various stages of the process flow can be seen in Figure 16.



**Figure 16. Visual process flow and progression of hardware leading into hot-fire testing.**

The hot-wall was post-processed using chemical milling and chemical mechanical polishing (CM/CMP). This process was selected due to concern that the nozzle would be slightly out of round following deposition and heat treatments and not feasible to machine to the tolerance required. Even if the nozzle were out of round by 0.005” (0.127 mm) this would require specialty tooling to allow even wall thickness removal by machining. This is not feasible nor is the cost warranted for this and thus the CM/CMP process was selected. Since the CM/CMP process is based on chemical milling, the out of roundness does not impact the final results. An image of the nozzle post hot-wall CMP is shown in Figure 17.



**Figure 17. Post chemical mechanical polishing (CMP) of the hot wall for improved surface finish and reduced total heat load performance.**

The test configuration for the LLAMA assembly included a GRCop-42 L-PBF chamber, L-PBF pentad injector, and compact augmented spark igniter (CASI) shown in Figure 18. There were separate inlets to the chamber and nozzle for CH<sub>4</sub> cooling. The chamber cooling entered the aft end and was routed to the forward end with direct flow into the injector. This test series included a series of integral instrumentation ports on the chamber for channel cooling

performance. The LP-DED nozzle had a facility line routed for the inlet and facility lines for the CH4 cooling exit, which was dumped to the burn stack.

The nozzle specifically included pressure and temperature for forward and aft manifolds to determine performance. The test series was sequenced so that multiple cycles could be obtained during a single test allowing for fully-reversal cyclical loads to be completed to challenge the hardware. The facility at TS115 allowed for four 15 second cycles with a 10 second purge and cool-down in-between cycles. The targeted chamber pressure was 750 psig (51.7 bar) and MR of 3.00. The nozzle was designed for a peak wall temperature of approximately 1,100°F (593°C).

The test assembly was checked out with appropriate blowdowns, igniter, and ignition tests before attempting full mainstage cycles. Mainstage tests were planned to operate at full chamber pressures to maximize thermal environments to the chamber. Each test was run as close to nominal test conditions as possible with considerations taken towards facility limits. A few facility limitations prevented testing exactly at the fully nominal values.

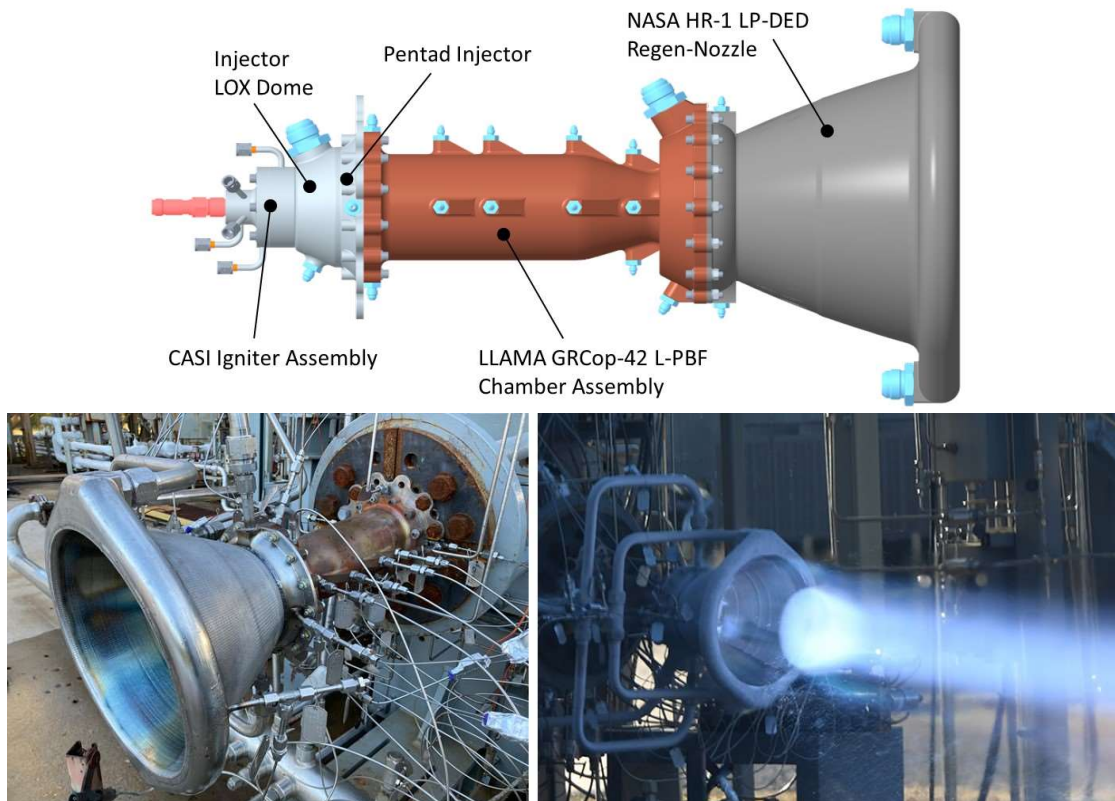


**Figure 18. LLAMA Test Assembly. (Top) TCA configuration and associated drawing numbers, (Left) LLAMA Test Assembly with LP-DED NASA HR-1 nozzle and GRCop-42 L-PBF chamber installed, (Right) Hot-fire testing of the assembly at MSFC TS115.**

There were two test series completed with the LP-DED regen nozzle assembled, which included PK058 and PK129. Both series used slightly different chambers, but with identical geometry and material on the hot-wall (GRCop-42) and coolant channels. A total of 40 tests were completed on the LP-DED NASA HR-1 nozzle accumulating 568.4 seconds. The pressure drop across the nozzle was very low and met expected modeling. Throughout the course of testing, varying degrees of bluing on the nozzle were observed (Figure 19), as expected, as the hot-wall was subjected to high temperatures. The bluing is generally indicative that the nozzle reached temperatures that were expected with predictions. The bluing observed on the nozzle is observed locally from some streaking with a higher degree at the interface just downstream of the chamber. The bluing at the forward end is expected with the higher expected heat fluxes. Overall, there were no indications of cracking or other failures indicating the temperatures were an issue.



**Figure 19. Bluing of the nozzle observed. (Left) LP-DED nozzle after 7 starts, (Right) Nozzle after 40 starts.**

## VII. Conclusions

The Fe-Ni hydrogen-resistant NASA HR-1 alloy using additive manufactured (AM) laser powder directed energy deposition (LP-DED) has matured through process development, material characterization and testing, manufacturing technology demonstrators (MTD) and component builds, and successful completion of hot-fire testing. NASA HR-1 is a high-temperature oxidation and corrosion resistant superalloy targeted for use in liquid rocket engine components, such as channel wall nozzles. The material has performed well in a relevant hot-fire test environment for an actively-cooled channel wall nozzle sized for 7K-lb<sub>f</sub> testing under the Long Life Additively Manufactured Assembly (LLAMA) and Rapid Analysis and Manufacturing Propulsion Technology (RAMPT) projects. The 7K-lb<sub>f</sub> nozzle achieved a total of 40 starts and 568 seconds with no issues noted and achieved a Technology Readiness Level (TRL) of 5/6. The hot-fire testing achieved a milestone for the material maturity and demonstrated excellent performance in a relevant environment. The nozzle design achieved a low pressure drop and performed well with wall temperatures exceeding 1,100°F.

NASA HR-1 alloy was demonstrated to be readily built using LP-DED and the process scaled up. The LP-DED processes allows for thin-wall and thick-wall deposition. A 65% RS-25 nozzle MTD was completed at a diameter of 58 inches (1.47 meters) and total height of 72 inches (1.83 meters) built in 90 days deposition time. This build time is a significant savings over traditional manufacturing techniques and the part count was brought down to less than 10. The MTD showed little distortion compared to the CAD model and successfully achieved all manufacturing objectives.

The NASA HR-1 has completed characterization and optimization of a heat treatment cycles, which includes stress relief, homogenization, solution and aging. The LP-DED NASA HR-1 exhibits expected trends in strength and ductility as temperatures of aging cycles are reduced and the improved strain hardening behavior that is important for low cycle fatigue. The tensile properties and the low cycle fatigue properties of additively manufactured LP-DED NASA HR-1 were observed to be lower than the wrought material with the standard heat treatment being used and with adjusted aging cycles, as expected. Further adjustments in the heat treatment cycles have been proposed to improve upon the issue of Ti segregation observed in LP-DED NASA HR-1 and mechanical testing to characterize these new heat treatment cycles are planned.

While channel wall nozzles with thin-wall structures were the target of the LP-DED process using NASA HR-1, several other components were fabricated using the technology. Overall, the NASA HR-1 has demonstrated capability within the LP-DED additive method, and additional material characterization and testing will be completed in addition to ongoing hot-fire testing at 1.2K-lb<sub>f</sub>, 7K-lb<sub>f</sub> and 40K-lb<sub>f</sub> thrust levels to obtain additional process and design data. Further testing of the NASA HR-1 7K nozzle is expected in 2021 using liquid oxygen (LOX) as the coolant in addition to high mixture ratios and low total mass flow rates through the nozzle. NASA is making mechanical and hot-fire data available to industry partners and working to actively mature the supply chain.

## Acknowledgements

This paper describes objective technical results and analysis. Any subjective views or opinions that might be expressed in the paper do not necessarily represent the views of the National Aeronautics and Space Administration (NASA) or the United States Government.

Several people are recognized in the advancement, testing, management, and funding to mature the NASA HR-1 alloy and subsequent processes. This work was funded by the National Aeronautics and Space Administration (NASA) specifically through the STMD Rapid Analysis and Manufacturing Propulsion Technology (RAMPT) Project and Space Launch System (SLS) Liquid Engines Office (LEO) supporting advancements in additive manufacturing. Thank you to our partners involved including RPM Innovations (RPMI), Auburn University, Rem Surface Engineering, Procam, PTR, TMC, Maximus Welding, and several others. We wish to thank the project offices for their support: John Fikes/RAMPT, Jessica Wood/LEO, Robert Hickman/LEO, and Johnny Heflin/LEO. Thank you to several individuals involved in testing – Tal Wammen, Scott Chartier, TS115 test crew, David Olive, and many others involved. Thank you to Design and analysis support from Shawn Skinner, Bob Witbrodt, Adam Willis, Jonathan Nelson, Rory Jones, Brandon Cook. Thank you to the team engaged in materials characterization and testing including Matt Medders, John Luke Bili, GRC team, Westmoreland Mechanical. There are also many other individuals involved from NASA and industry – thank you!

## References

- [1] Gradl, P. “Rapid Fabrication Techniques for Liquid Rocket Channel Wall Nozzles.” AIAA-2016-4771, Paper presented at 52nd AIAA/SAE/ASEE Joint Propulsion Conference, July 27, 2016. Salt Lake City, UT.
- [2] Gradl, P. R., & Protz, C. S. (2020). Technology advancements for channel wall nozzle manufacturing in liquid rocket engines. *Acta Astronautica*, 174, 148-158. <https://doi.org/10.1016/j.actaastro.2020.04.067>
- [3] Gradl, P.R., Greene, S.E., Brandsmeier, W., Johnston, I. Hot-fire Testing and Large-scale Deposition Manufacturing Development Supporting Liquid Rocket Engine Channel Wall Nozzle Fabrication, Paper presented at 65th JANNAF Propulsion Meeting/10th Liquid Propulsion Subcommittee, May 21-24, 2018. Long Beach, CA.
- [4] Kerstens, F., Cervone, A., Gradl, P. (2021). End to end process evaluation for additively manufactured liquid rocket engine thrust chambers. *Acta Astronautica*. 182, 454-465. <https://doi.org/10.1016/j.actaastro.2021.02.034>
- [5] Gradl, P., Greene, S., Protz, C., Bullard, B., Buzzell, J., Garcia, C., Wood, J., Osborne, R., Hulka, J. Cooper, K. Additive Manufacturing of Liquid Rocket Engine Combustion Devices: A Summary of Process Developments and Hot-Fire Testing Results. 54th AIAA/SAE/ASEE Joint Propulsion Conference, AIAA Propulsion and Energy Forum, (AIAA 2018-4625). July 9-12, 2018. Cincinnati, OH.
- [6] Gradl, P., Protz, C., Cooper, K., Garcia, C., Ellis, D., Evans, L. GRCop-42 Development and Hot-fire Testing using Additive Manufacturing Powder Bed Fusion for Channel-cooled Combustion Chambers. 55th AIAA/SAE/ASEE Joint Propulsion Conference, AIAA Propulsion and Energy Forum. August 19-21, Indianapolis, IN. AIAA-2019-4228
- [7] Gradl, P., Protz, C., Wammen, T. Additive Manufacturing Development and Hot-fire Testing of Liquid Rocket Channel Wall Nozzles using Blown Powder Directed Energy Deposition Inconel 625 and JBK-75 Alloys. 55th AIAA/SAE/ASEE Joint Propulsion Conference, AIAA Propulsion and Energy Forum. August 19-21, Indianapolis, IN. AIAA-2019-4362
- [8] Gradl, P., Protz, C., Fikes, J., Clark, A., Evans, L., Miller, S., Ellis, D.L., Hudson, T. Lightweight Thrust Chamber Assemblies using Multi-Alloy Additive Manufacturing and Composite Overwrap. AIAA Propulsion and Energy Forum. August 24-26. Virtual. (2020). AIAA-2020-3787.

- [9] ASTM International. (2016). *ASTM F3187 - 16 Standard Guide for Directed Energy Deposition of Metals*. ASTM.Org. <https://www.astm.org/Standards/F3187.htm>
- [10] Anderson, R., Terrell, J., Schneider, J., Thompson, S. and Gradl, P., 2019. Characteristics of Bi-metallic Interfaces Formed During Direct Energy Deposition Additive Manufacturing Processing. *Metallurgical and Materials Transactions B*, pp.1-10.
- [11] Oniuke, B., Heer, B. and Bandyopadhyay, A., 2018. Additive manufacturing of Inconel 718—copper alloy bimetallic structure using laser engineered net shaping (LENS™). *Additive Manufacturing*, 21, pp.133-140.
- [12] Bandyopadhyay, A. and Heer, B., 2018. Additive manufacturing of multi-material structures. *Materials Science and Engineering: R: Reports*, 129, pp.1-16.
- [13] Gradl, P., Protz, C., Wammen, T. “Additive Manufacturing Development and Hot-fire Testing of Liquid Rocket Channel Wall Nozzles using Blown Powder Directed Energy Deposition Inconel 625 and JBK-75 Alloys”. 55th AIAA/SAE/ASEE Joint Propulsion Conference, AIAA Propulsion and Energy Forum. August 19-22. Indianapolis, IN. (2019).
- [14] Gradl, P., Mireles, O. and Andrews, N., 2019. Introduction to Additive Manufacturing for Propulsion Systems. M19-7605. AIAA Propulsion and Energy Forum and Exposition; August 19, 2019 - August 22, 2019; Indianapolis, IN; United States. 10.13140/RG.2.2.13113.93285
- [15] Hauser, C. Additive Manufacturing Seminar: Blown Powder Activities. TWI Materials and Joining Technologies. Retrieved from: [www.twi-global.com/\\_resources](http://www.twi-global.com/_resources). (2015)
- [16] Karczewski, K., Peška, M., Ziętała, M. and Polański, M., 2017. Fe-Al thin walls manufactured by laser engineered net shaping. *Journal of Alloys and Compounds*, 696, pp.1105-1112.
- [17] K.S. Chan, M. Koike, R.L. Mason, and T. Okabe, Fatigue Life of Titanium Alloys Fabricated by Additive Layer Manufacturing Techniques for Dental Implants, *Metall. Trans. A.*, 2013, 44A, p 1010– 1022.
- [18] DebRoy, T., Wei, H.L., Zuback, J.S., Mukherjee, T., Elmer, J.W., Milewski, J.O., Beese, A.M., Wilson-Heid, A., De, A. and Zhang, W., 2018. Additive manufacturing of metallic components—process, structure and properties. *Progress in Materials Science*, 92, pp.112-224.
- [19] Sames, W.J., List, F.A., Pannala, S., Dehoff, R.R. and Babu, S.S., 2016. The metallurgy and processing science of metal additive manufacturing. *International Materials Reviews*, 61(5), pp.315-360.
- [20] P. S. Chen, B. Panda, and B.N. Bhat, ” NASA HR-1, A New Hydrogen Resistant Fe-Ni Base Superalloy”, Hydrogen Effects in Materials, edited by A.W. Thompson and N.R. Moody, Minerals, Metals, and Materials Society (TMS), 1996.
- [21] A.W. Thompson, J.A. Brooks, “Hydrogen Performance of Precipitation-Strengthened Stainless Steels Based on A-286.” *Metallurgical Transactions A*, Vol. 6, No. 7, 1975, p. 1431. doi:10.1007/BF02641935.
- [22] P.S. Chen, C.C. Katsarelis, W.M. Medders, P.R. Gradl, “Segregation Evolution and Diffusion of Titanium in LP-DED NASA HR-1”, NASA/TM–20210013649.
- [23] M. Morinaga, N. Yukawa, and H. Adachi, “Alloying Effect on the Electronic Structure of Ni<sub>3</sub>Al (γ’),” *J. Phys.Soc. Japan*, 1984, vol. 53, No. 2, pp.653-63.
- [24] M. Morinaga, N. Yukawa, H. Ezaki, “Solid Solubilities in Transition-Metal Based FCC Alloys,” *Phil. Mag. A*, 51 (1985), No. 2, pp.223-246.

- [25] M. Morinaga, N. Yukawa, and H. Adachi, and H. Ezaki, "New PHACOMP and Its Application to Alloy Design," *Superalloys*, 1984, edited by M. Gell, M.C.S. Kortovich, R.H. Bricknell, W. B. Kent and J.F. Radavich, The Metallurgical Society of AIME , 1984, pp.523-532.
- [26] M. Morinaga, N. Yukawa, and H. Adachi, "Alloying Effect on the Electronic Structure of BCC Fe," *J. Phys.F: Met. Phys.* 15 (1985), pp. 1071-1084
- [27] P. R. Gradl, T. W. Teasley, C. S. Protz, and C. C. Katsarelis, P. P. Chen. (2021). Hot-fire Testing Results of Additively Manufactured NASA HR-1 towards Large Scale Implementation of Channel Wall Nozzles. 68th JANNAF Propulsion Meeting (JPM) / 12th Liquid Propulsion (LPS) / Joint Subcommittee Meeting. Virtual. June 7-11.
- [28] "η-Phase TTP Diagram Development for LP-DED NASA HR-1," Internal Research, NASA Marshall Space Flight Center, Huntsville, AL.
- [29] "Progress in Thermal Process Development and Ti Segregation Mitigation for AM NASA HR-1," Internal Research, NASA Marshall Space Flight Center, Huntsville, AL.
- [30] Katsarelis, C., Chen, P., Gradl, P., Protz, C., Jones, Z., Ellis, D., and Evans, L. Additive Manufacturing of NASA HR-1 Material for Liquid Rocket Engine Component Applications. *JANNAF Dec.* 2019.
- [31] Chen, P., and Mitchell, M. "ALLOY NASA-HR-1." No. April 2005, 2005.
- [32] Gradl, P.R., Protz, C. "Large-Scale Channel Wall Nozzle Development using DED and LWDC Additive Manufacturing Techniques." Paper presented at 2019 JANNAF 11th Liquid Propulsion Subcommittee (LPS), December 9-13. Tampa, FL. (2019).
- [33] Gradl, P. R., Protz, C., Fikes, J., Clark, A., Evans, L., Miller, S., Ellis, D., & Hudson, T. (2020). Lightweight thrust chamber assemblies using multi-alloy additive manufacturing and composite overwrap. *AIAA Propulsion and Energy 2020 Forum*, 1–25. <https://doi.org/10.2514/6.2020-3787>